Appendix 1

ARMA 12-330

Creep Behavior of Barnett, Haynesville, and Marcellus Shale

Li, Yawei
Texas A&M University, College Station, TX, USA
Ghassemi, Ahmad
Texas A&M University, College Station, TX, USA

Copyright 2012 ARMA, American Rock Mechanics Association

This paper was prepared for presentation at the 46th US Rock Mechanics / Geomechanics Symposium held in Chicago, IL, USA, 24-27 June 2012.

This paper was selected for presentation at the symposium by an ARMA Technical Program Committee based on a technical and critical review of the paper by a minimum of two technical reviewers. The material, as presented, does not necessarily reflect any position of ARMA, its officers, or members. Electronic reproduction, distribution, or storage of any part of this paper for commercial purposes without the written consent of ARMA is prohibited. Permission to reproduce in print is restricted to an abstract of not more than 300 words; illustrations may not be copied. The abstract must contain conspicuous acknowledgement of where and by whom the paper was presented.

ABSTRACT: In order to assess the contribution of creep to closure rate and conductivity loss of hydraulic fractures in gas shale, the visco-elastic characteristics of gas shale have been investigated. A series of creep tests were conducted on gas shale core samples. First, a few uniaxial creep tests were performed on several selected samples, and then multi-stage triaxial creep tests were carried out at room temperature. Samples used in the tests come from three different gas shale reservoirs. It is found that the creep strain can be described by a power-law function of time. The clay and carbonate contents of these shale samples vary noticeably, and it is observed that rocks with more cement and less clay have higher elastic modulus, Pseudo-steady state creep rate increases linearly with deviator stress and higher confining pressures increase the amount of creep strain under the same deviator stress.

1. INTRODUCTION

Achieving economic production in nano-Darcy permeability gas-shale reservoirs requires creating a large surface area by hydraulic fracturing. However, many factors contribute to the loss of productive fracture area and the reduction of fracture conductivity, both immediate and over time. These lead to low flow rates, low recovery, and often marginal or uneconomical production. Proppant and asperity embedment into fracture surface under constant closure stress is a major cause of reduction of fracture conductivity. The in-situ stress normal to the fracture surface acts on the proppants and the asperities between the two fracture faces. The rock at the fracture faces tends to creep with time. This is enhanced by fracturing fluid and high temperature. The issue of viscous flow/creep has been considered but data and creep models need be developed for better understanding its contribution to permeability loss. Fracture closure is controlled by the elastic, plastic and viscous property of the shale formation.

The elastic closure response occurs instantaneously when the net effective minimum horizontal stress increases as a result of reservoir depletion. The elastic response to close the fracture follows Hooke's law of elasticity and is controlled by Young's modulus of the formation. The early stage of fracture closure is governed more by the elastic property of the shale formation, but the creep become significant to fracture closure with time.

The creep (viscous) effect is a slow, time-dependent deformation. The total deformation obtained from applying a constant stress is the sum of two components, deformation resulting from elastic response and the creep function. The creep function characterizes the rheological properties of the shale formation and is best described experimentally for a given stress range, temperature, water content and lithology.

To evaluate the influence of the elastic, plastic and viscous property of shale formation on the fracture conductivity reduction, experimental research work needs to be performed on shale to obtain its visco-elasto-plastic property of both core sample scale and proppant size scale in simulated subsurface environment (temperature, water content etc.).

To investigate the visco-elasto-plastic property of the shale samples from the Barnett, Marcellus, and Haynesville shale formations, a series of multistage tri-axial creep experiments were performed at various differential stresses and confining pressures. A multistage creep test enables us to obtain creep parameters at different stress-state from a single core sample by applying a step-wise loading path. The initial

sets of test have been conducted at room temperature. However, test under reservoir temperature conditions are ongoing and will be reported at a later time.

2. EXPERIMENT DESCRIPTION

2.1. Sample Description

Plugs from Barnett, Marcellus and Haynesville have been tested. The Barnett sample 3-20 is from a depth of 5552.35ft, while the Marcellus sample 09-30 is from a depth of 5899.48ft, Haynesville samples 05-21 and 05-22 come from depths of 12424.75ft and 12454.55ft. The mineral content of the four samples and their elastic modulus are listed in Table 1. The samples were prepared for testing by TerraTek-Shlumberger core preparation laboratory. All samples were drilled perpendicular to apparent bedding.

All samples were kept under room humidity condition prior to the test and experiments were conducted under dry and drained condition, in this way we were able to eliminate poro-elastic effects, so the data represents the behavior of the dry rock. All samples are 1" in diameter and they all have the standard 1 by 2 aspect ratio except Marcellus 09-20 (2.09" length).

Table.1.Mineral contents of the four samples, QFP refers to quartz, feldspar, plagioclase, and pyrite component

Sample name	QFP %	Carbonate %	Clay %	Others %
Marcellus 09-30 5899.48ft	28	9	40	24
Barnett 3-20 5552.35ft	60	10	25	5
Haynesville 05-21 12454.75ft	25	23	33	18
Haynesville 05-22 12454.75ft	25	23	33	18

Table.2. Young's modulus of the four samples (perpendicular to bedding) at different confining pressures

Sample name	Confining pressure MPa	Young's modulus GPa
Marcellus 09-30	19	17.2
	16	15.5
	5	12.7
Barnett 3-20	16	32.1
	0	27.8
Haynesville 05-21	0	14.5
Haynesville 05-22	16	17.6

Fig.1.The four shale samples used for the creep test

2.2. Experimental Procedures

All the creep tests were performed on GCTS triaxial rock test system, two additional Teledyne syringe pumps were used to provide constant confining pressure and axial load, axial load is applied to the samples with a hydraulic cylinder (hydraulic jack). The loading paths of the four samples are listed in Table 2. After installing the sample and displacement sensor assembly in the confining cell, a constant confining pressure is applied first, and then the sample is loaded with a desired deviator stress (constant) for a desired period of time. The deviatoric stress is then increased to a higher value if required, and is held constant. During this process, the deformation of the sample is monitored and recorded. A typical multistage loading path & the axial strain response are illustrated in Fig.4.

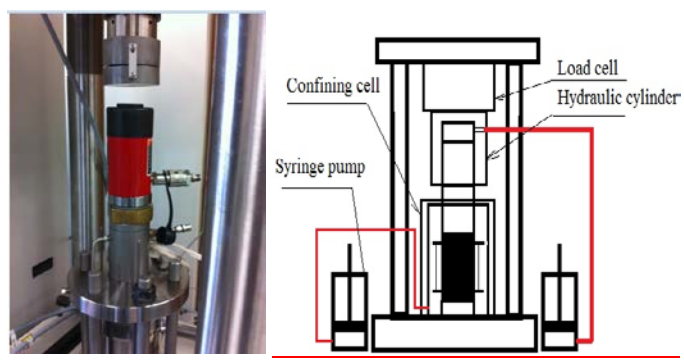

Fig.2. Hydraulic cylinder for axial load, schematic drawing of the creep test setup.

Table.3. Loading path of the four samples

Sample name	Confining pressure MPa	Deviator stresses MPa
Marcellus 09-30	16	27-36
	19	55-64-72-81-89
	5	64
Barnett 3-20	16	46.5-53.5-63-73-83
	0	45-55-64-72-81
Haynesville 05-21	0	34-45-63.5-72
Haynesville 05-22	16	36.4-55-64

3. TEST RESULT AND INTERPRETATION

For the Marcellus 09-30 sample, the first applied confining pressure is 16 MPa and was applied using the GCTS pressure booster. For the first two stages, the confining pressure was around 16 MPa but in the middle of the two stages test it gradually increased to 19 MPa (not planned). To maintain consistency, the confining pressure of all later stages was kept at 19 MPa using a more stable Teledyne ISCO pump.

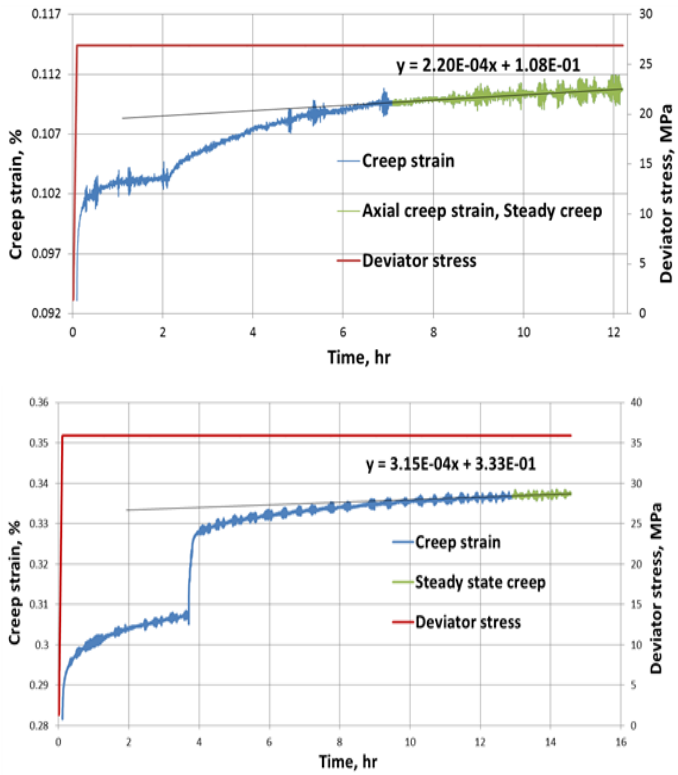

Fig.3.The first two stages of creep tests on Marcellus 09-30.

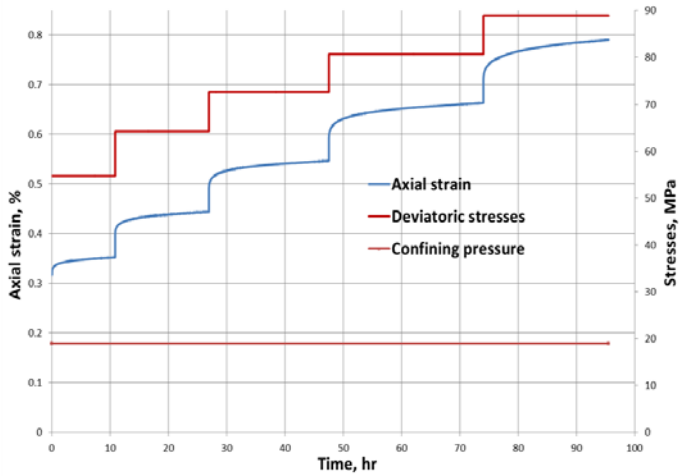

Fig.4. The loading path & the axial strain of Marcellus 09-30, 3rd to 7th stage.

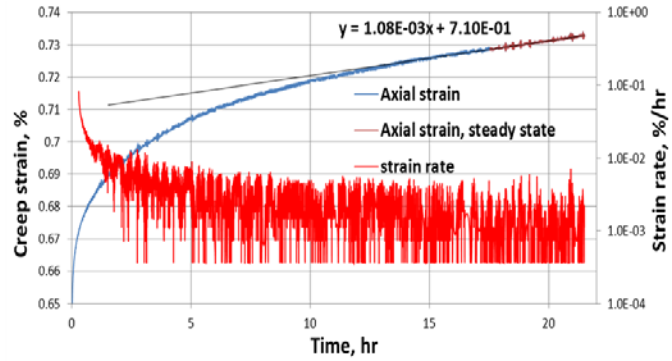

Fig.5.The axial creep strain and strain rate of Marcellus 09-30, the 7th stage.

For the creep strain of a constant stress stage, the strain rate $d\varepsilon_1/dt$ decreases with time until a constant value is reached. However, the strain-time curve does not completely level off. A similar result has been reported by Zoback et al [1] for unconsolidated GOM shale that was tested for 6 days. Thus, we only use the last portion of the strain-time curves and consider it as a quasi-steady-state strain. The strain rates of the 1st to 7th stage of creep test were obtained by fitting a strain line to the last portion of the strain-time curves, as shown in Fig. 5. The strain rate-stress relation is plotted in Fig. 6.

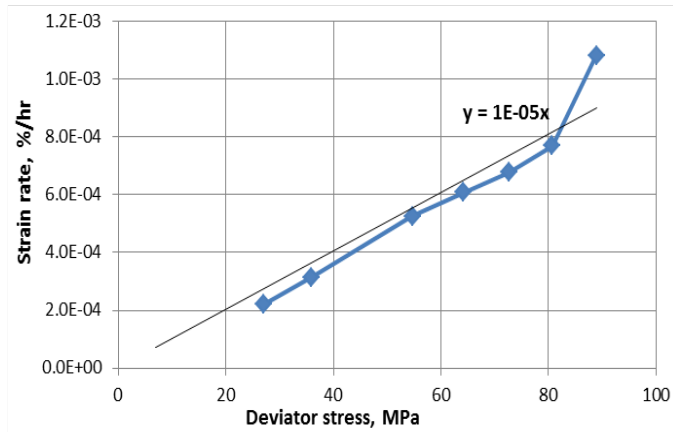

Fig.6.Strain rate-stress relation for Marcellus 09-30 at a confining pressure of 19 MPa,

As shown in Fig.6, the quasi-steady strain rate increases almost linearly with deviator stress. At higher deviator stress, the trend deviates from a linear relation indicated by the last point in Fig.6, implying a non-linear strain rate-stress relationship at higher deviatoric stresses; higher deviatoric stresses are not applied for fear of breaking the sample. In the 0-80 MPa range, the creep can be modeled using a linear visco-elastic model such as Burgers and Maxwell. But because the Maxwell model is not able to capture the transient creep portion of the strain-time relation, Burgers model is used to model this multistage creep. Because the confining pressure of the first two stages jumped from 16MPa to 19 MPa, the first two stages are neglected when fitting the data with Burgers model. A least-square fitting method was used

to fit Burgers model (Eq.1) to the strain-time curve obtained from 3rd to 7th stage creep, and the four parameters are summarized in Table.4.

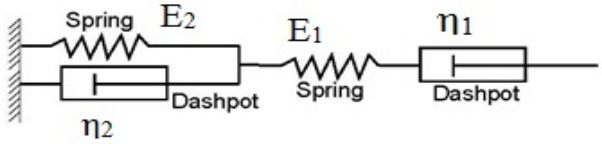

Fig.7. Four element Burgers model.

$$\varepsilon = \frac{\sigma}{E_1} + \frac{\sigma}{\eta_1} t + \frac{\sigma}{E_2}\left(1 - e^{-\frac{E_2}{\eta_2}t}\right) \quad (1)$$

$$\frac{d\varepsilon}{dt} = \frac{\sigma}{\eta_1} + \frac{\sigma}{\eta_2} e^{-\frac{E_2}{\eta_2}t} \quad (2)$$

In which E_1 is the time independent young's modulus of the rock, E_2 determines the amount of primary creep strain.

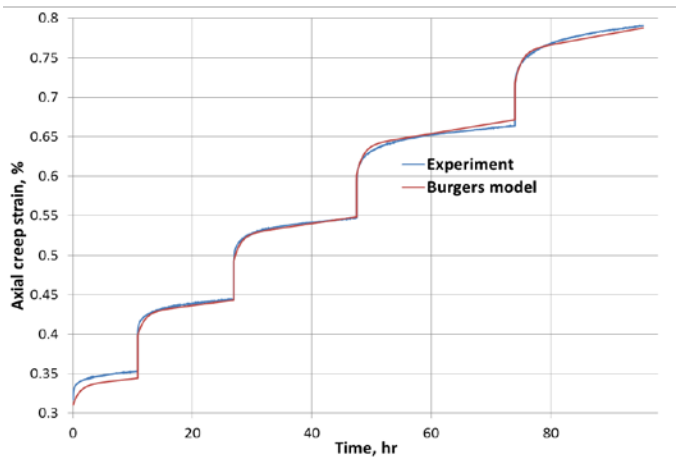

Fig.8.Comparisons between real creep strain and Burger creep reaction, confining pressure 19MPa.

The two elastic and viscous parameters were obtained using the least-square fitting method. As can be seen, the Burgers model gives a relatively good fit to the creep data.

Table.4. Burger creep parameters, perpendicular to bedding

	E1,GPa	E2,GPa	η_1, Pa·s	η_2, Pa·s
Marcellus09-30 (19MPa)	17.624	221.041	2.32E+10	8.87E+08
Barnett03-20 (16MPa)	32.735	2443.63	9.46E+10	9.75E+09
Haynesville (16MPa)	17.296	322.203	1.36E+11	3.21E+09

The power law (power function of stress and time) has been widely used by various researchers to express stress-strain-time relationships for nonlinear viscoelastic materials [2, 3]. It has the following form which is often called the nutting equation:

$$\varepsilon^c = k\sigma^p t^n \quad (3)$$

ε^c is the creep strain without the instantaneous elastic strain, because the quasi-strain rate increases almost linearly with deviator stress, thus p=1, the total strain of a constant stress creep test is:

$$\varepsilon = \frac{\sigma}{E} + k\sigma t^n \quad (4)$$

Similarly, a least-square fitting method was used to fit creep law model (Eq.4) to the strain-time curve obtained from 3rd to 7th stage creep, and the three parameters are summarized in Table.5.

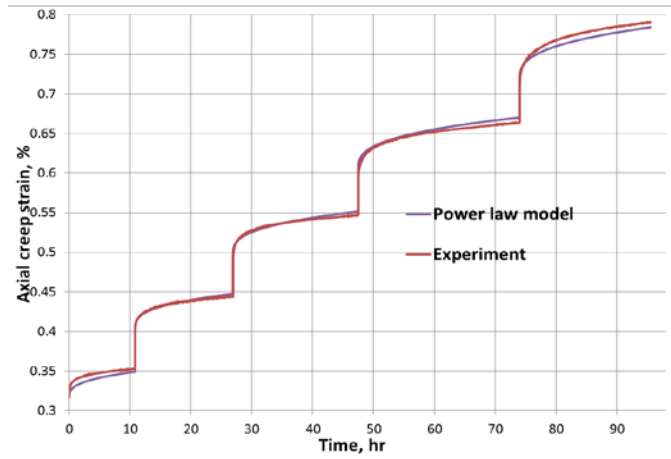

Fig.9.Comparisons between real creep strain and power law creep reaction, confining pressure 19MPa.

Table.5. Power law creep parameters, perpendicular to bedding

	E , GPa	k	n
Marcellus09-30 (19MPa)	17.246	2.55E-04	0.349379
Barnett03-20 (16MPa)	33.246	4.53E-05	0.349379
Haynesville (16MPa)	17.384	1.03E-04	0.473279

Similarly, the data of Barnett 03-20 and Haynesville 5-22 are processed, and the parameters are summarized in Table 4-5.

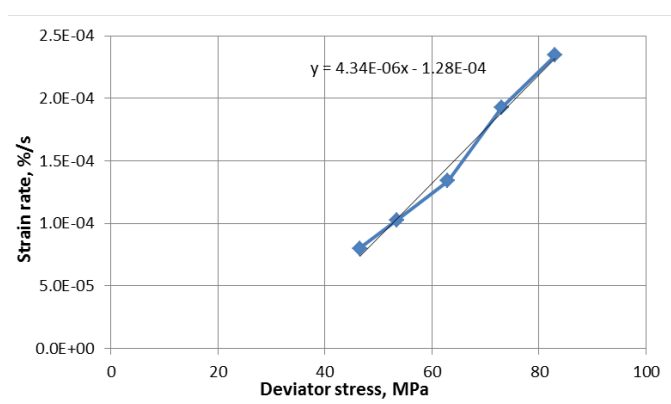

Fig.10. Strain rate-stress relation, confining pressure 16 MPa, Barnett 03-20.

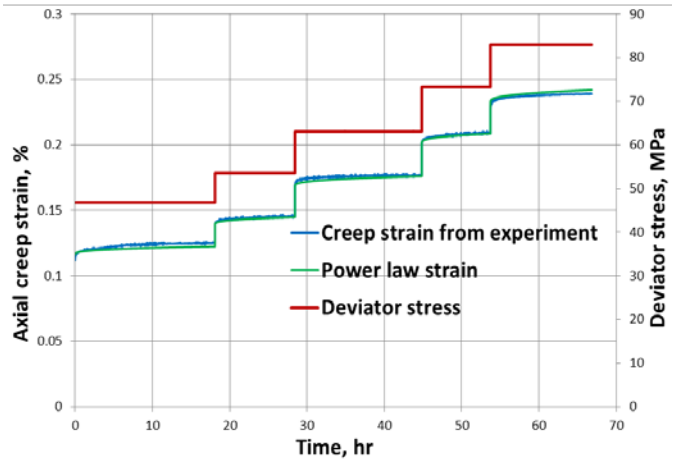

Fig.11. Comparisons between real creep strain and power law creep reaction to five stresses, confining pressure 16MPa, Barnett 3-20.

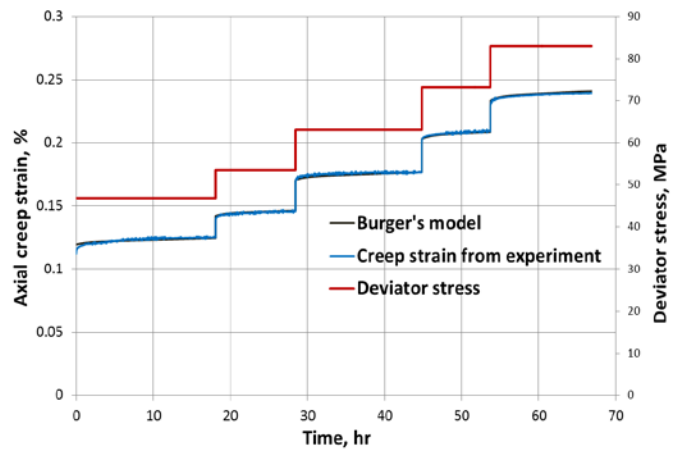

Fig.12. Comparisons between real creep strain and power law creep reaction to five stresses, confining pressure 16MPa, Barnett 3-20.

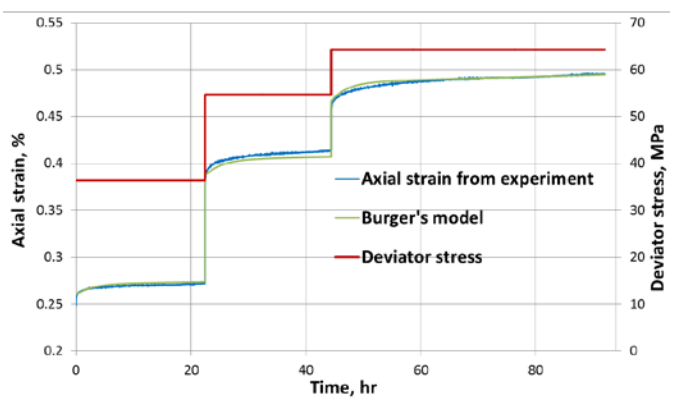

Fig.13. Comparisons between real creep strain and Burger's creep reaction to three stresses, confining pressure 16MPa, Haynesville 5-22.

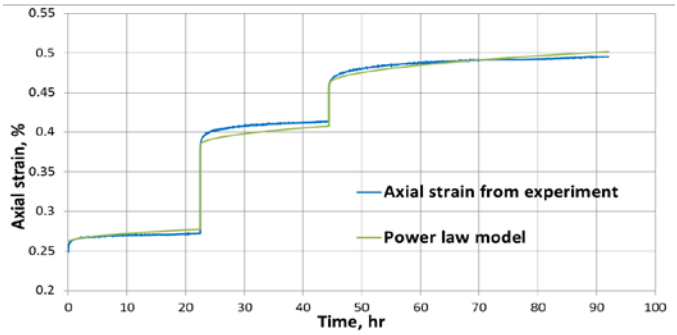

Fig.14. Comparisons between real creep strain and power law creep reaction to three stresses, confining pressure 16MPa, Haynesville 5-22.

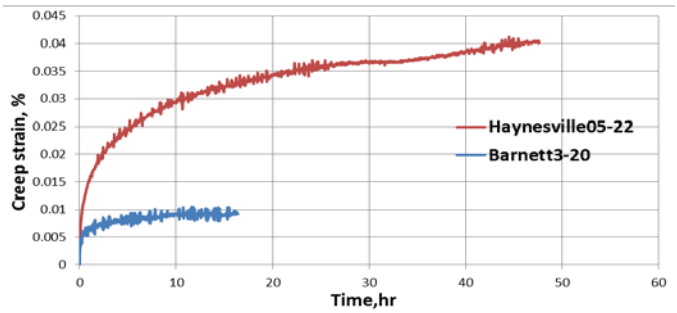

Fig.15. Comparisons between two creep strain under the same confining pressure 16MPa and the same deviator stress 63MPa, all creep strain are taken to zero by subtracting the elastic strain for better comparison.

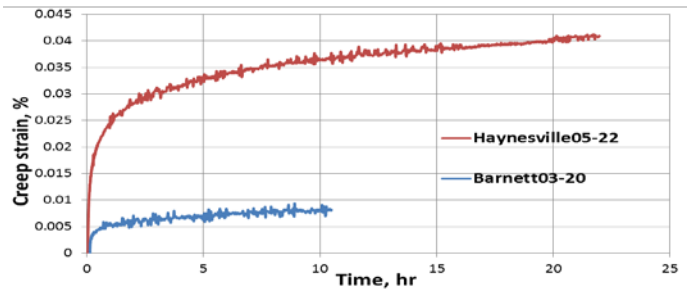

Fig.16. Comparison between two creep strain under the same confining pressure 16MPa, and the same deviator stress 55MPa.

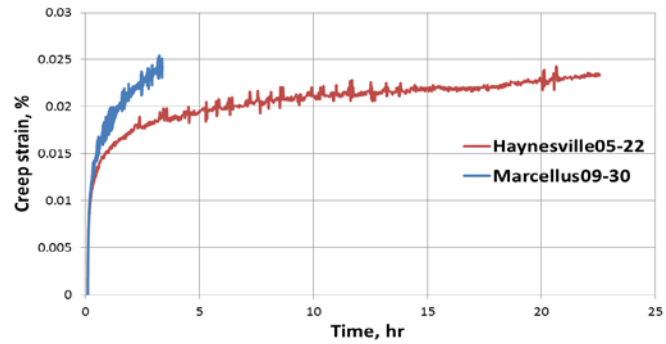

Fig.17. Comparison between two creep strain under the same confining pressure 16MPa, and the same deviator stress 36MPa, for Marcellus sample, the portion of confining pressure jumping to 19 MPa was removed.

From Fig.15-17, with the knowledge of Young's modulus and clay content, one can tell that a stiffer shale (less clay) creeps less under the same stress state and ambient conditions.

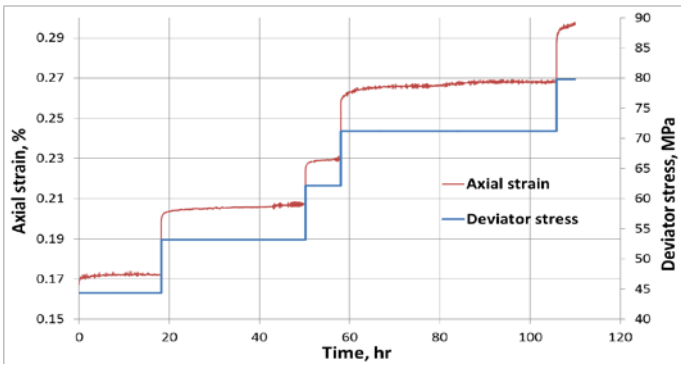

Fig.18. The multistage loading path & the axial strain of Barnett 3-20, confining pressure is 0 MPa.

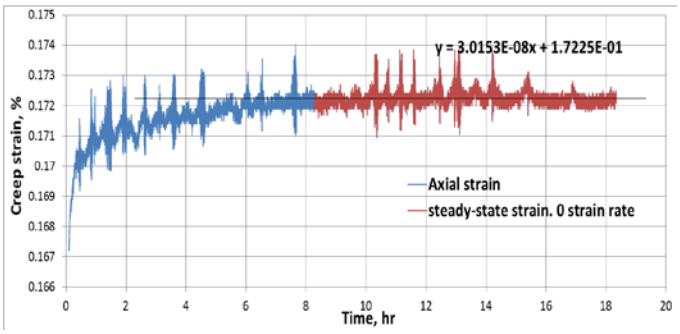

Fig.19. Creep strain and strain rate of Barnett 3-20, at Deviator stress 46.5MPa.

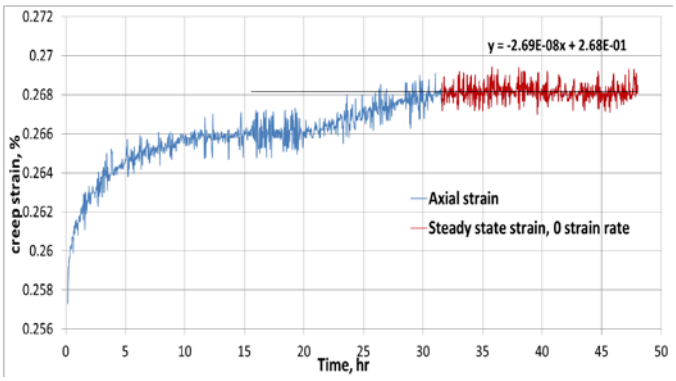

Fig.20. Creep strain and strain rate of Barnett 3-20, at Deviator stress 73MPa.

For uniaxial creep of Barnett 3-20, the strain rates of three creep stages show zero strain rates (it cannot be negative except at strain recovery). The last stage is not long enough to show the strain rate of steady-state creep.

Through the above observation, one can postulate that the uniaxial creep of Barnett 03-20 has a stress threshold for steady state creep. Below this stress, there is no steady-state creep (the strain-time curve is flat at the end); while above this stress one can observe the steady-state creep with slopes.

4. INFLUENCE OF CONFINING PRESSURE

The amount of creep strain depends on confining pressure. It has been reported that for salt, the amount of creep strain decreases with increasing confining pressure [4]. However, in this study the opposite trend is found. For the same sample, two creep stages with the same deviator stress but different confining pressures are compared in Figs. 21-26.

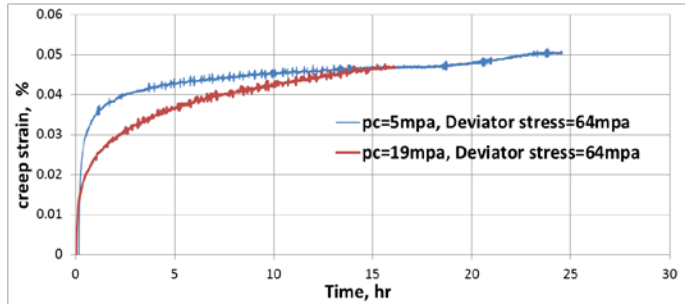

Fig.21. Comparisons of creep strain under the same deviator stress at two confining pressures, Marcellus 09-30.

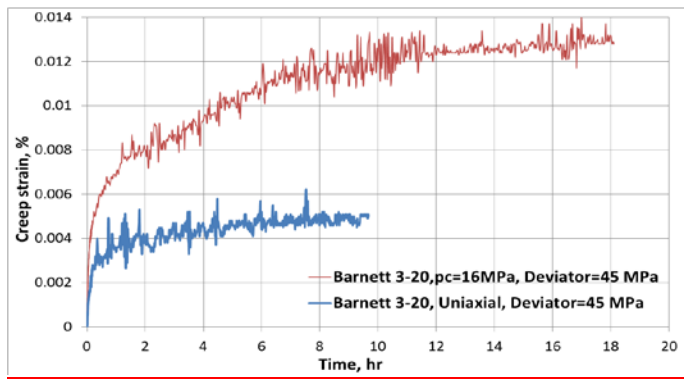

Fig.22. Comparisons of creep strain under the same deviator stress 45MPa at two confining pressures, Barnett 3-20, 1st stage.

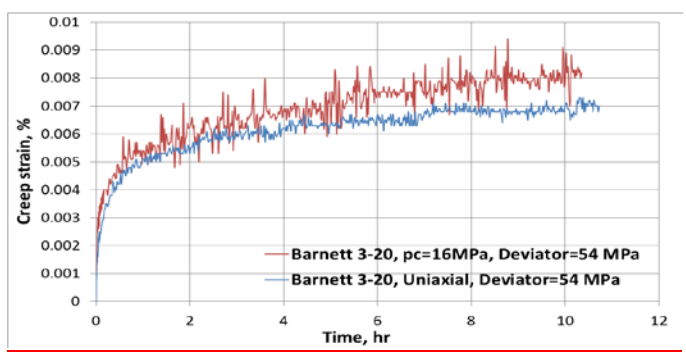

Fig.23. Comparisons of creep strain under the same deviator stress 54MPa at two confining pressures, Barnett 3-20, 2nd stage.

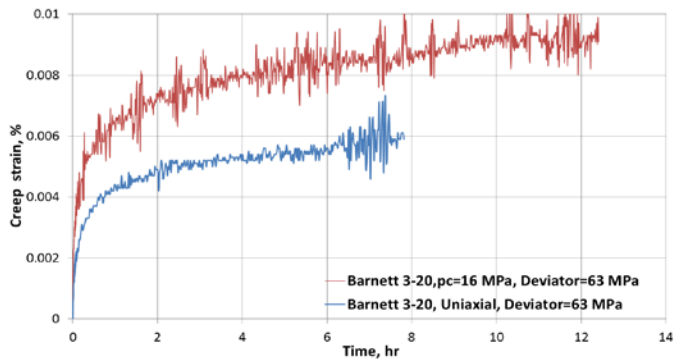

Fig.24. Comparisons of creep strain under the same deviator stress 63MPa at two confining pressures, Barnett 3-20, 3rd stage.

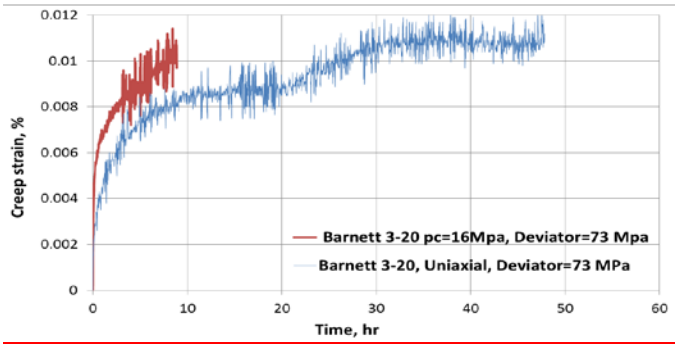

Fig.25. Comparisons of creep strain under the same deviator stress 73MPa at two confining pressures, Barnett 3-20, 4th stage.

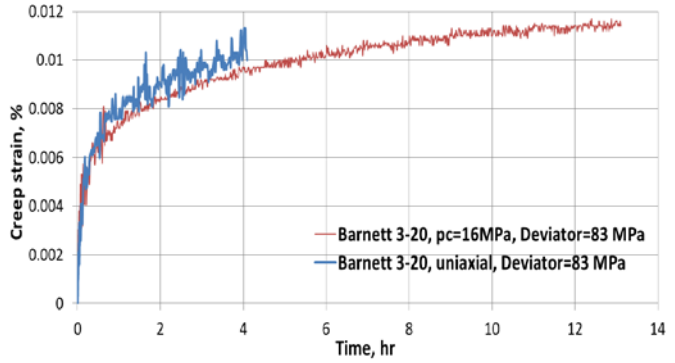

Fig.26. Comparisons of creep strain under the same deviator stress 83MPa at two confining pressures, Barnett 3-20, 5th stage.

It is interesting to notice that higher confining pressure increases the amount of creep strain at a certain time under the same deviator stress. The only exception is Fig. 26 for deviatoric stress 83 MPa. We speculate that when the deviatoric stress is greater than the stress threshold for steady-state creep, the creep strain for uniaxial stress becomes larger than that of triaxial stress condition.

5. DISCUSSION

A series of creep tests were conducted on gas shale core samples. The tests included uniaxial creep tests, and multi-stage triaxial creep tests all at room temperature. Samples used in the tests come from four three different gas shale reservoirs. The clay and carbonate content of these shale samples vary noticeably.

Our results show that stiffer shale creeps less while shale with higher amounts of clay and organic material creep more. It implies that Young's modulus and clay content is a good indicator for the relative difference in viscoelastic property. Young's modulus correlates well with mineralogical composition. Shale with more clay and less quartz has a smaller Young's modulus.

For uniaxial creep, a deviator stress threshold exists, below that stress threshold, the steady-state strain rate is zero; above that stress threshold, the sample exhibits steady-state creep.

The power law function of stress and time describes the creep deformation well for the shale samples tested under the reported conditions of room temperature. Burgers model can also be used to describe the creep strain response. Burgers model is a strictly viscoelastic creep model and excludes plastic deformation and microcracking. To consider the effect of plasticity and microcracking, a more general creep constitutive equation needs to be formulated. Further studies on the behavior of these rocks under in-situ conditions (confining pressure, temperature, humidity) and more detailed consideration of mineralogy are ongoing.

REFERENCES

1. Chang, C and Zoback, M.D. 2008. Creep in unconsolidated shale and its implication on rock physical properties. In *42th US Rock Mechanics Symposium, San Francisco, CA, June 29-July 2, 2008, 08-130.*
2. William N. Findley., James S.Lai, and Kasif Onaran.1976. *Creep and relaxation of nonlinear viscoelatic material.* 2nd ed. North-holland publishing company, 8-10.
3. Hagin, P.N and Zoback, M.D. 2010. Inverting for creep strain parameters of uncenmented reservoir sands using arbitrary stress-strain data. In *44th US Rock Mechanics Symposium, Salt Lake City, 27-30 June 2010, 10-171.*
4. Chunhe Yang, J.J.K. Daemen and Jian-Hua Yin. 1999. Experimental investigation of creep behavior of salt rock. *International Journal of Rock Mechanics and Mining Sciences* 36 (1999) 233±242